Weak ferromagnetism and domain effects in multiferroic $LiNbO_3$-type $MnTiO_3$-II

Angel M. Arévalo-López and J. Paul Attfield*

Centre for Science at Extreme Conditions and School of Chemistry, University of Edinburgh, Mayfield Road, Edinburgh EH9 3JZ United Kingdom

(Received 7 May 2013; revised manuscript received 7 August 2013; published 18 September 2013)

Magnetic order consistent with multiferroism has been observed in the acentric $LiNbO_3$-type, high pressure form II of $MnTiO_3$ using neutron diffraction and magnetization measurements. Spin order below the 28 K magnetic transition has propagation vector (0 0 0), and spins lie in the *ab* plane. Representation symmetry analysis shows that the antiferromagnetic Mn^{2+} spin component observed by neutron scattering, of magnitude 3.9(1) μ_B at 2 K, coexists with a weak ferromagnetic component of magnitude 0.0014 μ_B. This magnetization is perpendicular to the electrical polarization resulting from cation displacements in this acentric structure, permitting coupled switches of the two ferroic orders. The spin order is stable to fields of at least 5 T; however, facile domain reorientation within the *ab* plane enhances the antiferromagnetic susceptibility and a constant magnetization/field (M/H) is observed in field strengths greater than ~1.5 T. Suppression of the {101} neutron intensity with field follows the same Brillouin-dependence as M/H and enables the antiferromagnetic easy axes to be identified as parallel to the *ab* plane hexagonal axes.

DOI: 10.1103/PhysRevB.88.104416 PACS number(s): 75.25.−j, 75.47.Lx, 75.85.+t, 75.30.Kz

I. INTRODUCTION

The couplings between magnetic and ferroelectric orders in multiferroic materials are of fundamental physical interest and may also have applications in memory technologies,[1–3] for example, to write magnetic data using electric fields. Within transition metal oxides, magnets require *d* electrons to form localized magnetic moments, whereas d^0 cations are a common source of polar distortions that give rise to ferroelectricity.[4] Hence, materials that contain both d^0 and magnetic d^n cations are of interest for the observation of magnetoelectric couplings, and $MnTiO_3$ based on $3d^0$ Ti^{4+} and $3d^5$ spin $S = 5/2$ Mn^{2+} is an attractive candidate.

At ambient pressure, $MnTiO_3$ forms a centrosymmetric, ilmenite-type polymorph that undergoes a spin-flop transition at a critical field of ~6 T leading to magnetoelectricity and a proposed ferrotoroidal order.[5] A high pressure polymorph $MnTiO_3$-II can be quenched to ambient conditions,[6,7] and this adopts an acentric $LiNbO_3$-type structure and is a potential multiferroic material. The polar lattice distortion was recently predicted to induce weak ferromagnetism in spin-ordered $LiNbO_3$-type $ATiO_3$ (A = Fe, Mn, and Ni) phases through the antisymmetric Dzyaloshinsky-Moriya (DM) exchange interaction, leading to a proposed mechanism for the electric field control of magnetization.[8] Coexistence of weak ferromagnetism and ferroelectricity in $LiNbO_3$-type $FeTiO_3$ and magnetodielectric coupling in $MnTiO_3$-II have subsequently been reported,[9,10] but the magnetic structures were not determined. We report here a neutron and magnetization study of the low temperature spin order in $MnTiO_3$-II in zero and applied magnetic fields, leading to the discovery of an unusual low field domain reorientation which breaks the powder-averaging diffraction and allows an unambiguous determination of the spin directions.

II. EXPERIMENTAL

Polycrystalline, ilmenite-type $MnTiO_3$-I was prepared by firing MnO and TiO_2 at 1200 °C. Small charges were transformed to the $LiNbO_3$-type form II polymorph [space group $R3c$, 300 K lattice parameters: $a = 5.2023(1)$ Å and $c = 13.6856(2)$ Å] under 8 GPa pressure at 1000 °C using a Walker-type multianvil apparatus. The analogous phase $MnVO_3$ adopts a perovskite structure under these conditions,[11] but no $MnTiO_3$-perovskite was observed in our high pressure studies. Six products that were found to be pure $MnTiO_3$-II by powder x-ray diffraction were combined to give a ~70 mg sample for powder neutron diffraction experiments.

The magnetization of $MnTiO_3$-II powder was measured on a Quantum Design superconducting quantum interference device (SQUID) magnetometer. Variable temperature data were collected under zero-field-cooled (ZFC) and field-cooled (FC) conditions from 2 to 300 K in a 0.5 T applied field. The zero-field spin order in $MnTiO_3$-II was determined using neutron diffraction data from diffractometer D20 at the Institut Laue-Langevin (ILL) facility. Profiles were recorded between 2 and 50 K at a wavelength of 2.418 Å. Neutron scattering as a function of applied magnetic field strength was studied on the Wish spectrometer at the ISIS neutron facility.[12] The sample was cooled to 2 K, and data were collected in fields between 0 and 5 T. No demagnetization corrections were made to the data reported here.

III. RESULTS AND DISCUSSION

A. Magnetic structure

Magnetic susceptibility measurements for $MnTiO_3$-II in a 0.5 T field are similar to those in a previous report[9] and show an ordering transition at $T_M = 28$ K with divergence between FC and ZFC curves and Curie-Weiss paramagnetism at higher temperatures (Fig. 1).[13] A fit to inverse susceptibility data between 100 and 300 K gives a paramagnetic moment of 6.1(1) μ_B, close to the theoretical value of 5.92 μ_B for localized $S = 5/2$ Mn^{2+} and a Weiss temperature of $\theta = -171(1)$ K showing that antiferromagnetic spin-spin interactions are dominant but are partially frustrated with a moderate value of the frustration factor $|\theta|/T_M \approx 6$.

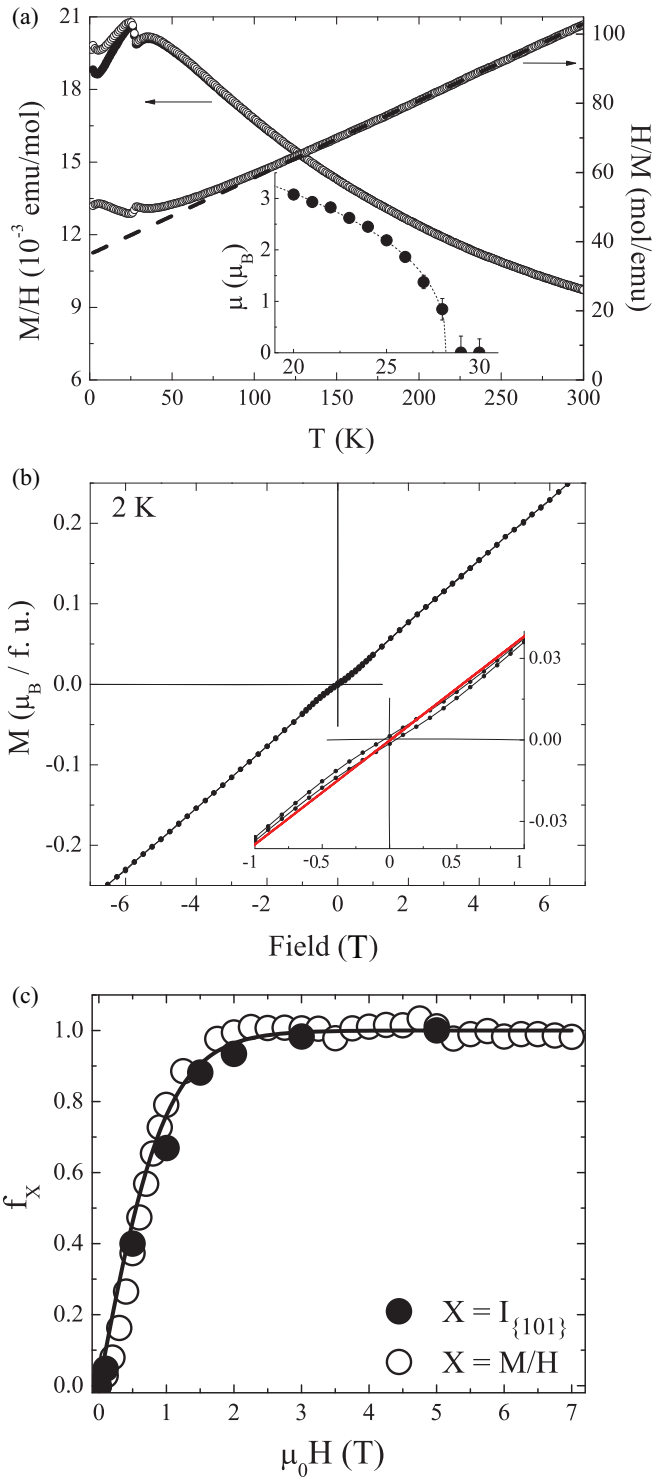

FIG. 1. (Color online) (a) Evolution of the direct and inverse magnetic susceptibilities of $MnTiO_3$-II with temperature under a 0.5 T field showing the 28 K spin-ordering transition (open/filled points are FC/ZFC data). The inset displays the temperature variation of the ordered Mn moment from neutron diffraction, showing the critical law fit described in the text. (b) M-H loop from cycling between ± 7 T fields at 2 K. Inset displays the low field hysteresis with a superimposed line showing the high field constant M/H limit. (c) Normalized variations of M/H from the initial magnetization experiment and of the $\{101\}$ magnetic neutron intensity with the fit of the $S = \frac{1}{2}$ Brillouin function.

TABLE I. Refinement results (atomic coordinates and thermal B-factors, bond lengths, and BVS's) for $MnTiO_3$-II at 2 K from ILL D20 powder neutron diffraction data [space group $R3c$; $a = 5.1878(1)$ Å, $c = 13.6791(6)$ Å; residuals $R_p = 3.12\%$, $R_{wp} = 5.31\%$, $R_{exp} = 1.51\%$].

	x	y	z	B_{iso} (Å^2)
Mn	0	0	0.284(2)	0.45(1)
Ti	0	0	0	0.28(3)
O	0.0602(9)	0.337(2)	0.068(2)	0.23(1)

Bond	Length (Å)	Bond	Length (Å)
Mn-O ($x3$)	2.29(3)	Ti-O ($x3$)	2.03(2)
Mn-O ($x3$)	2.13(1)	Ti-O ($x3$)	1.90(2)
	Mn	Ti	O
BVS	2.02(5)	4.09(7)	2.03(5)

Magnetization (M)-field (H) measurements below T_M are consistent with a weakly ferromagnetic ground state, as a hysteretic variation with a saturated weak ferromagnetic magnetization (taken from the remnant magnetization) of $M_{WFsat} = 0.0014\ \mu_B$/Mn is observed [Fig. 1(b)]. This is in good agreement with the predicted value of 0.002 μ_B/f.u. for $MnTiO_3$ (see Ref. 8). However, an unusual M-H behavior is observed as the slope increases at low fields and tends to a constant M/H value above 1.5 T. This is seen by plotting the normalized function $f_X(H) = (X - X_{H\to 0})/(X_{H\to\infty} - X_{H\to 0})$ for the variable $X = M/H$, as shown in Fig. 1(c), and is further discussed in terms of domain effects later.

The crystal and zero-field magnetic structures of $MnTiO_3$-II were determined using powder neutron diffraction data at a constant wavelength of 2.418 Å; structure refinement results are shown in Table I. Polar displacements of both cations parallel to the c axis are evident from their bond distances to oxygen. Possible cation inversion disorder between Mn and Ti could not be directly investigated as their neutron scattering lengths are very similar, but the bond valence sums (BVSs) in Table I indicate that Mn^{2+} and Ti^{4+} are fully ordered with no evidence for cation inversion.

Two prominent magnetic neutron diffraction peaks, indexed as $\{003\}$ and $\{101\}$, appear at temperatures below 28 K (Fig. 2) and are consistent with a $\boldsymbol{k} = (0\ 0\ 0)$ propagation vector. Representation analysis of the $MnTiO_3$-II magnetic order was performed using the BasIreps program within the FULLPROF suite.[14] The irreducible representations (IrReps) and the associated basis vectors for possible (0 0 0) spin orders are summarized in Table II. The Γ_1 and Γ_2 IrReps, respectively, define antiferro- and ferromagnetic spin orders parallel to $\boldsymbol{c}$, and neither accounts for the observed magnetic diffraction intensities. The Γ_3 IrRep contains four basis vectors that describe antiferro- and ferromagnetic spin orders in the ab plane. For later convenience, we use vectors that each contain moments from only one of the two Mn spins, but basis sets with linear combinations of both spins derived through a similarity transformation may also be used. Combinations of Γ_3 basis vectors that describe antiferromagnetic order of Mn spins give a good fit to the magnetic neutron diffraction data [Fig. 2(c)]. Moments are parallel in each plane and

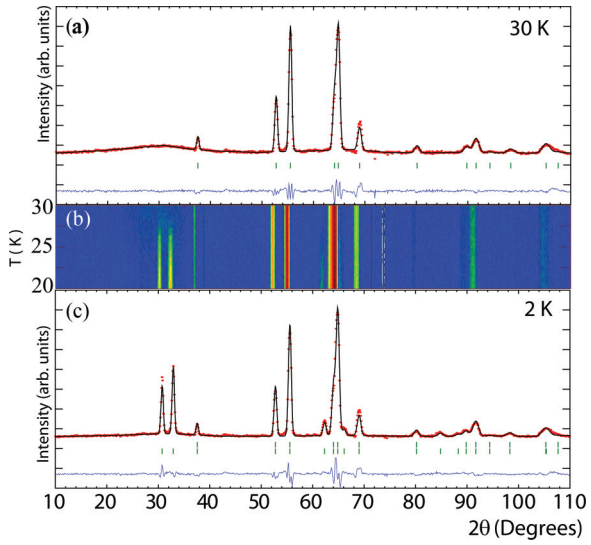

FIG. 2. (Color online) Powder neutron diffraction data for $MnTiO_3$-II. (a) Fit of the nuclear structure to the 30 K profile. (b) Scattering intensity plots (dark/light shading shows low/high neutron counts) between 20 and 30 K, showing the appearance of magnetic diffraction peaks below 28 K. (c) Fit of the nuclear and magnetic structures (upper and lower tick marks, respectively) to the 2 K profile.

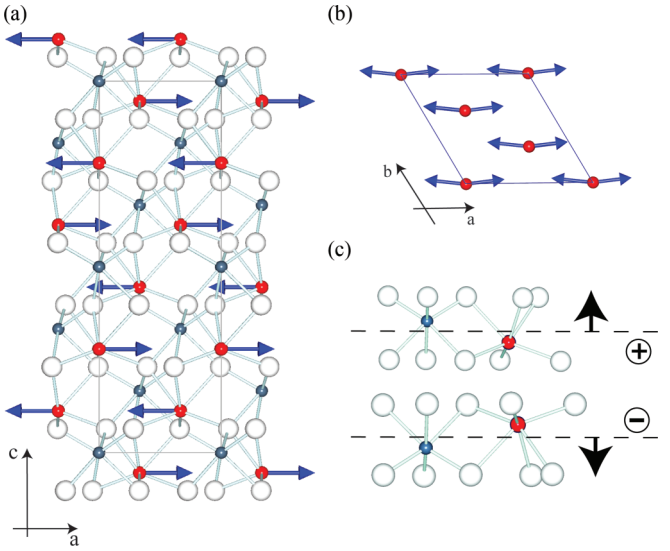

FIG. 3. (Color online) Crystal and magnetic structures of $MnTiO_3$-II. (a) Mn spin order in the ac plane. (b) (001) projection of the magnetic structure with antiferromagnetic components shown parallel to the a axis, and the perpendicular weak ferromagnetic component (not to scale) parallel to the [120] direction. (c) The possible perpendicular-switching mechanism proposed in Ref. 8, where inversion of the Mn and Ti displacements as electrical polarization is changed from the $+\boldsymbol{c}$ direction (upper image) to $-\boldsymbol{c}$ (lower image), switches the magnetization in (b) from [120] to the $[\bar{1}\bar{2}0]$ direction.

antiparallel to moments in adjacent planes [Fig. 3(a)], although the spin directions in the ab plane are not determined in this experiment. The refined magnetic moment of 3.9(1) μ_B at 2 K is significantly lower than the ideal value of 5 μ_B expected for $S = 5/2$ Mn^{2+}, in agreement with geometric frustration evidenced from the magnetization measurements. Contributions from other vectors that belong to the same Γ_3 IrRep are allowed by symmetry, and these describe the weak ferromagnetic component that arises from antisymmetric DM exchange. Refinement gave the upper magnitude of this ferromagnetic component as 0.3 μ_B, perpendicular to the directions of the antiferromagnetic spins (equivalent to a 4° canting of the 3.9 μ_B moments), but no statistically significant improvement to the fit was obtained.

The fit of a critical law $\mu(T) = \mu(0)[1 - (T/T_M)]^{\beta}$ to the refined values of magnetic moment μ in the temperature range $20 < T < 28$ K is shown in Fig. 1(a) and gives $T_M = 28.2(2)$ K and $\beta = 0.38(2)$. The critical exponent is close to the theoretical value of $\beta = 0.34$ for a three-dimensional XY magnet, which is appropriate to $S = 5/2$ Mn^{2+} spins lying in the ab plane of an anisotropic material.

TABLE II. Irreducible representations and basis vectors for Mn spin order in $MnTiO_3$-II for the $\boldsymbol{k} = (0\ 0\ 0)$ propagation vector in space group $R3c$. Mn1 and Mn2 correspond to spins at (0, 0, 0.284) and (0, 0, 0.784), respectively.

		Mn1			Mn2		
IrRep	Basis vectors	m_x	m_y	m_z	m_x	m_y	m_z
Γ_1	ψ_1	0	0	1	0	0	−1
Γ_2	ψ_2	0	0	1	0	0	1
Γ_3	ψ_3	3/2	0	0	0	0	0
Γ_3	ψ_4	0	0	0	−3/2	−3/2	0
Γ_3	ψ_5	0	0	0	$-\sqrt{3}/2$	$\sqrt{3}/2$	0
Γ_3	ψ_6	$-\sqrt{3}/2$	$-\sqrt{3}$	0	0	0	0

The observed spin structure of $MnTiO_3$-II validates the perpendicular magnetoelectric switching mechanism proposed in Ref. 8, where the ferroelectric polarization **P** is parallel to the c axis, and the net magnetization **M** is in the ab plane, shown parallel to the [120] direction in Fig. 3(b). If **P** is switched from the $+\mathbf{c}$ to the $-\mathbf{c}$ direction using an electric field, the consequent inversion of the Ti and Mn displacements [Fig. 3(c)] should lead to a coupled switch of **M** from the [120] to the $[\bar{1}\bar{2}0]$ direction. The combination of **P**, **M**, and the direction of the antiferromagnetic spin components also introduces chirality to the spin structure of $MnTiO_3$-II, although the $LiNbO_3$-type arrangement is polar but nonchiral.

B. Domain effects

To give insights into the unusual M-H behavior of $MnTiO_3$-II, the magnetic neutron scattering at 2 K was studied as a function of applied magnetic field on the Wish spectrometer at the ISIS neutron facility. No new magnetic peaks were observed up to a field of 5 T. As shown in Figs. 4(a) and 4(b), the intensity of the {101} magnetic diffraction peak $I_{\{101\}}$ decreases with applied field and saturates at 52% of the zero-field value above ∼1.5 T, whereas the {003} intensity is unchanged. The normalized $f_X(H)$ variation of $X = I_{\{101\}}$ on Fig. 1(c) closely follows that of $X = M/H$, demonstrating a common physical origin for the unusual evolution of magnetization and the suppression of $I_{\{101\}}$ with applied magnetic field. Rietveld fits to the zero field, and 5 T neutron data shown in Fig. 4(c) confirm that the decrease

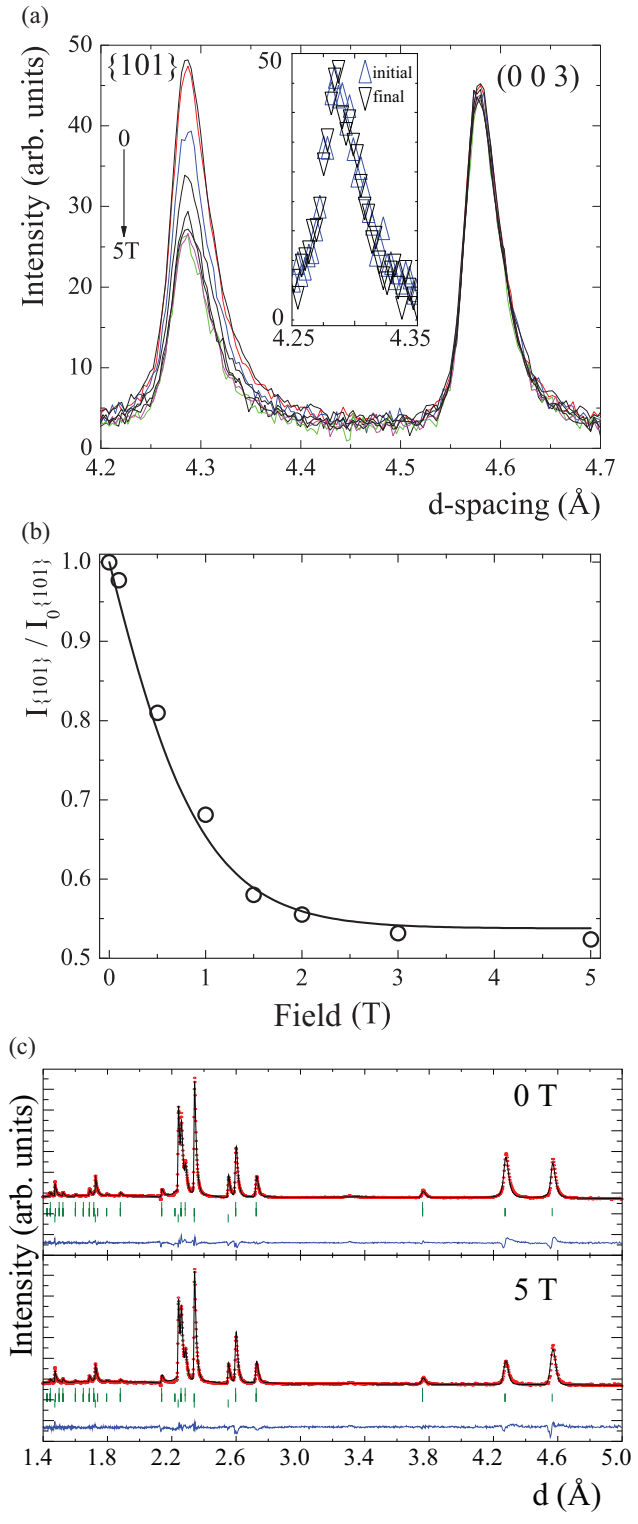

FIG. 4. (Color online) (a) Magnetic powder neutron diffraction intensities of $MnTiO_3$-II as a function of applied field at 2 K. The inset shows $\{101\}$ intensity in zero field before and after a 2 T field was applied, demonstrating that no sample texturing occurs. (b) Normalized variation of the $\{101\}$ intensity with field. (c) Rietveld fits of the crystal and magnetic structures of $MnTiO_3$-II to the zero field and 5 T diffraction profiles as described in the text, with a parasitic scattering contribution from aluminum shown by the lower Bragg markers.

of $I_{\{101\}}$ is the only apparent change in the applied field spectra. This effect was modeled by applying a standard texture (preferred orientation) function $\exp(-A\psi^2)$ to the magnetic intensities in the Rietveld refinements, where ψ is the acute angle between the scattering vector and the c axis, and the magnitude of fitting variable A increases with field.

In many cases, it is not possible to fit powder neutron diffraction patterns from magnetic materials in applied fields as changes in spin structure, sample texture, and domain orientation can all affect the intensity of magnetic scattering relative to zero-field data. However, $MnTiO_3$-II presents a relatively simple case, as most of these effects do not occur. The absence of new magnetic superstructure peaks and, of the large intensity changes expected for a transition to another $\boldsymbol{k} = (0\,0\,0)$ phase, shows that the magnetic structure is unchanged in fields up to 5 T, although the analysis presented later evidences a small increase in spin-canting angle. Texturing due to mechanical alignment of grains within the powder by the field would be evidenced by differences in magnetic diffraction intensities between zero-field spectra collected before and after a high field is applied. Similar high field Wish experiments, for example, on CoV_2O_6 (see Ref. 15), resulted in some texturing, but the field-induced change to $I_{\{101\}}$ for $MnTiO_3$-II is fully reversible to within counting errors [see Fig. 4(a) inset], so no texturing occurs here. This is attributed to the very small magnetization of weakly ferromagnetic $MnTiO_3$-II grains in comparison to the ferrimagnetic and ferromagnetic high field phases of CoV_2O_6. Hence, the field-induced change to $I_{\{101\}}$ for $MnTiO_3$-II is attributed to domain effects as the weakly ferromagnetic spin structure [Fig. 2(b)] can be switched between three equivalent easy axes in the ab plane. The resulting changes in magnetic diffraction intensities are consistent with the explanation that follows.

Powder diffraction peaks from high symmetry materials often sum over contributions from related (hkl) planes $\mathbf{h}$ that have equal d spacings but inequivalent structure factors $\mathbf{F_h}$. The intensity of a magnetic reflection is proportional to the square of the modulus of the magnetic interaction vector, which is the component of the magnetic structure factor perpendicular to the scattering vector $\boldsymbol{\varepsilon}$; $\mathbf{F}^{\mathrm{mag}}{}_{\mathbf{h}^\perp} = -(e^2\gamma/m_ec^2)\Sigma\ \mathbf{S}_{j^\perp} f_j \exp(2\pi i \mathbf{h}.\mathbf{r}i_j)$, summed over perpendicular spin components $\mathbf{S}_{j^\perp}$ at positions $\mathbf{r}_j$ in the unit cell, where f_j is the magnetic form factor (including the Debye-Waller term) and γ is the magnetic moment of the neutron. Canting of moments in $MnTiO_3$-II is very small, so only the antiferromagnetic spin components $\mathbf{S}_{\mathrm{AF}}$ give rise to appreciable neutron diffraction peaks. The perpendicular spin components $\mathbf{S}_{\mathrm{AF}^\perp}$ have magnitude $S_{\mathrm{AF}}\cos\alpha_{\mathrm{AF}}$, where α_{AF} is the acute angle between $\mathbf{S}_{\mathrm{AF}^\perp}$ and $\mathbf{S}_{\mathrm{AF}}$, as shown on Fig. 5(a), so diffraction intensity is proportional to $\cos^2\alpha_{\mathrm{AF}}$. Magnetic diffraction peaks in a powder pattern have contributions from families of related planes, for example, (101), $(\bar{1}11)$, and $(0\bar{1}1)$ planes contribute to the $MnTiO_3$-II magnetic $\{101\}$ intensity. The spin structure of $MnTiO_3$-II makes equivalent contributions to the magnetic interaction vector for these three planes except for their α_{AF} angles, so their relative intensities vary in proportion to $\cos^2\alpha_{\mathrm{AF}}$. Variations in $\cos^2\alpha_{\mathrm{AF}}$ for the three $\{101\}$ planes as a function of the angle φ between $\mathbf{S}_{\mathrm{AF}}$ and cell vector $\mathbf{a}$ are shown in Fig. 5(b). The average value of $\cos^2\alpha_{\mathrm{AF}}$ for the three

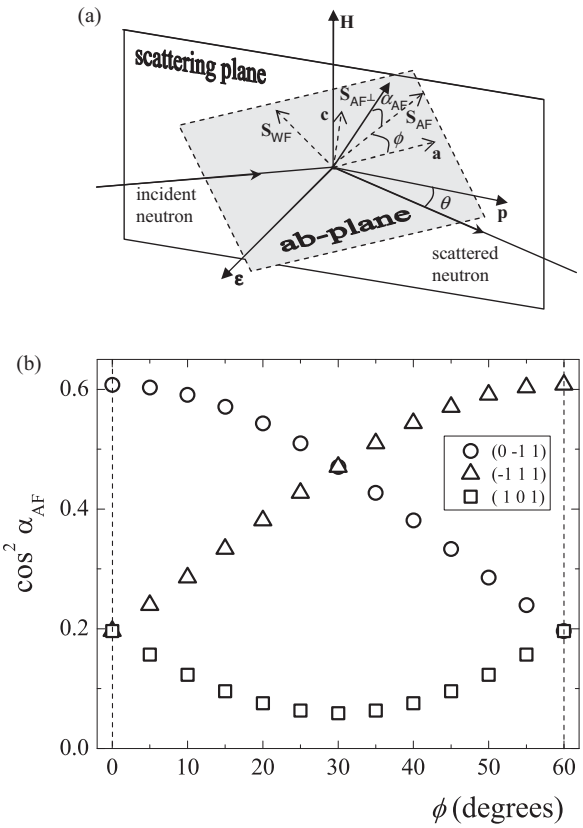

FIG. 5. (a) Scheme for the magnetic neutron diffraction experiment on $MnTiO_3$-II showing a Mn spin at the intersection of the (*hkl*) scattering plane and the *ab* plane of the crystal structure. Scattering vector $\boldsymbol{\varepsilon}$ is normal to the vertical magnetic field **H** and to **p** which is defined as the horizontal vector in the scattering plane. Vectors relevant to the *ab* plane are shown as broken lines; unit cell vector **c** is normal to this plane. Perpendicular antiferromagnetic $\mathbf{S}_{AF}$ and weak ferromagnetic $\mathbf{S}_{WF}$ spin components lie in the *ab* plane, and the offset of $\mathbf{S}_{AF}$ from unit cell vector **a** is represented by angle ϕ. Magnetic neutron intensities are determined by antiferromagnetic spin component in the scattering plane $\mathbf{S}_{AF^\perp}$, which makes acute angle α_{AF} to $\mathbf{S}_{AF}$. Domain switching rotates $\mathbf{S}_{AF}$ and $\mathbf{S}_{WF}$ by $\pm 120^\circ$ in the *ab* plane, which changes the magnitude of $\mathbf{S}_{AF^\perp}$ for some reflections. (b) Calculated variation of $\cos^2\alpha_{AF}$ with *ab* plane rotation angle ϕ for the $\{101\}$ family of scattering planes.

planes is $\frac{1}{3}$ for all φ angles in a zero-field experiment on a random powder. This illustrates the general restriction that spin directions in the *ab* plane of uniaxial materials cannot be found from powder-averaged magnetic neutron diffraction data.

When the magnetic easy axis for a ferro- or ferrimagnet is parallel to one of several otherwise equivalent directions in a high symmetry material, then domain reorientation by an applied magnetic field (without mechanical particle realignment) can change the powder diffraction intensities. This was demonstrated for a magnetite (Fe_3O_4) powder in early neutron scattering experiments where quantitative changes to the diffraction intensities as a result of ferrimagnetic domain reorientation were calculated.[16] The analysis is different for $MnTiO_3$-II because domain reorientation results from alignment of the weak ferromagnetic spin components $\mathbf{S}_{WF}$ by applied field **H**, whereas neutron diffraction measures the projection of the antiferromagnetic spin components $\mathbf{S}_{AF}$ on the scattering plane as $\mathbf{S}_{AF^\perp}$. $\mathbf{S}_{WF}$ and $\mathbf{S}_{AF}$ are mutually perpendicular and lie in the *ab* plane. Domain reorientation changes their directions by $\pm 120^\circ$ in this plane as there are three equivalent easy-axis directions. The relationships between the spin components, field direction, unit cell vectors, and scattering-vector $\boldsymbol{\varepsilon}$ (which is normal to the scattering plane) are shown in Fig. 5(a). This construction is used to account for the field dependencies of $\{003\}$ and $\{101\}$ intensities in Figs. 4(a) and 4(b) as follows.

The $\{003\}$ family has only the (003) plane, and this represents a special case as here the scattering plane is parallel to the *ab* plane so both $\mathbf{S}_{WF}$ and $\mathbf{S}_{AF}$ are perpendicular to $\boldsymbol{\varepsilon}$ and $\mathbf{S}_{AF^\perp} = \mathbf{S}_{AF}$ (as $\alpha_{AF} = 0$). Application of the field will reorient domains between their three available *ab* plane directions so that $\mathbf{S}_{WF}$ is as close as possible to the **H** direction; hence, $\mathbf{S}_{AF}$ is close to the perpendicular direction **p**. However, such reorientations do not change α_{AF} (which is always zero), so the $\{003\}$ magnetic diffraction intensity does not change with applied field, as observed experimentally in Fig. 4(a).

$\boldsymbol{\varepsilon}$ is not parallel to **c** for the planes within the $\{101\}$ family, so the applied field changes populations of domains with different $\cos^2\alpha_{AF}$ values, and hence the composite $I_{\{101\}}$ magnetic diffraction-intensity changes. Domain reorientations bring $\mathbf{S}_{WF}$ toward the **H** direction and result in $\mathbf{S}_{AF}$ lying toward the perpendicular **p** or $\boldsymbol{\varepsilon}$ directions. The latter corresponds to the maximum value of α_{AF} (for a given plane and unknown *ab* plane rotation angle ϕ) so that $\cos^2\alpha_{AF}$ and hence $I_{\{101\}}$ are reduced in this experiment where **H** is perpendicular to $\boldsymbol{\varepsilon}$. The quantitative change in $I_{\{101\}}$ can be predicted from Fig. 5(b) as the $\cos^2\alpha_{AF}$ values for the three $\{101\}$ planes with a fixed spin orientation are equivalent to the values for the three possible spin domain orientations for a specific plane. The intensity reduction depends on the in-plane angle φ, which has a domain of unique solutions for $0 \leqslant \varphi \leqslant 30^\circ$. The two highest symmetry candidate spin structures have $\varphi = 0$ and $\varphi = 30^\circ$. For $\varphi = 0$, two degenerate domain orientations [with the smallest $\cos^2\alpha_{AF} = 0.197$ value in Fig. 5(b)] bring $\mathbf{S}_{WF}$ closest to the **H** direction, and only these domains are populated at high field strengths. $I_{\{101\}}$ is thus predicted to fall to $3 \times 0.197 = 59\%$ of the zero-field value. At $\varphi = 30^\circ$, a unique domain orientation with $\cos^2\alpha_{AF} = 0.06$ is favored at high fields, leading to a predicted 18% of the zero-field $I_{\{101\}}$ value. The observed reduction of $I_{\{101\}}$ to 52% of the zero-field value at 5 T in Fig. 4(b) agrees well with the $\varphi = 0$ prediction. These models assume that the magnitudes of $\mathbf{S}_{WF}$ and $\mathbf{S}_{AF}$ do not change in applied field so the discrepancy between the $\varphi = 0$ prediction and the observed intensity reduction evidences a small field-induced canting of spins, which reduces S_{AF} and hence further diminishes $I_{\{101\}}$.

The above analysis shows that the reduction in $\{101\}$ magnetic neutron diffraction intensity and the insensitivity of $\{003\}$ are both consistent with reorientation of domains of antiferromagnetically aligned moments, driven by the interaction of their perpendicular weak ferromagnetic components with the applied field. Quantitative analysis of the $\{101\}$ intensity reduction is useful as it enables the spin direction within the *ab* plane to be determined for $MnTiO_3$-II. The $\varphi = 0$ antiferromagnetic structure shown in Fig. 3(b) is described by the $\psi_3 = -(\psi_4 + \sqrt{3}\psi_5)/2$ combination of bases from

Table II, and the perpendicular weak ferromagnetic component is given by $\psi_3 + \sqrt{3}\psi_6 = \psi_4 - \sqrt{3}\psi_5$.

The $f_X(H)$ field dependence of the normalized $I_{\{101\}}$ magnetic-neutron intensity and bulk M/H in Fig. 1(c) is fitted well by the Brillouin function $f_X(H) = B(H) = [(2S+1)/2S]\coth\{[(2S+1)/2S]H\} - (1/2S)\coth[(1/2S)H]$ for spin value $S = \frac{1}{2}$, as shown. The physical significance of this variation is unclear as domain magnetizations do not generally follow a Brillouin function, but it may reflect the availability of just two $\cos^2\alpha_{AF}$ values for the $\varphi = 0$ spin structure, as shown in Fig. 5. The close correspondence between the two $B(H)$ field variations is because $I_{\{101\}}$ and the bulk magnetization M $(=M_{WF} + M_{AF})$ in the direction of the applied field both vary linearly with the population difference between domain orientations. M_{WF} is very small in $MnTiO_3$-II so the M_{AF} magnetization contribution from reorientation of the antiferromagnetic spin components contributes significantly to M. The susceptibility of the collinear $\mathbf{S}_{AF}$ antiferromagnetic spin components is anisotropic and is greater in the perpendicular ($\mathbf{S}_{WF}$) direction than parallel to $\mathbf{S}_{AF}$. Hence, as the weak ferromagnetic moments of $MnTiO_3$-II are rotated toward the applied field direction, increasing M_{WF}, then the antiferromagnetic moments rotate into the perpendicular direction [see Fig. 3(b)], leading to an increase in M/H, which follows the same $B(H)$ variation as $I_{\{101\}}$.

IV. CONCLUSIONS

The $LiNbO_3$-type phase II of $MnTiO_3$ has been prepared by high pressure transformation of the ilmenite-type phase I at 8 GPa and studied by neutron and magnetization measurements. Mn^{2+} $S = 5/2$ spin order in the ab plane below 28 K appears antiferromagnetic by powder-neutron diffraction but is consistent with weak ferromagnetism through symmetry-allowed antisymmetric exchange driven by the DM interaction. The weak ferromagnetic component is perpendicular to the c axis electrical polarization and has been predicted to result in a strong magnetoelectric coupling.[8] The magnetic structure is stable to fields of at least 5 T; however, domain reorientation within the ab plane is facile and gives a pronounced enhancement to the antiferromagnetic susceptibility in moderate applied fields. Suppression of the $\{101\}$ neutron intensity with field follows the same Brillouin-dependence as M/H and enables the antiferromagnetic easy axes to be identified as parallel to the ab plane hexagonal axes.

ACKNOWLEDGMENTS

We acknowledge EPSRC and STFC for support and the provision of ILL and ISIS beam time and the Leverhulme Trust for additional support. We thank C. Ritter and M. Brunelli (ILL) and P. Manuel and D. Khalyavin (ISIS) for assistance with diffraction measurements.

*Corresponding author: j.p.attfield@ed.ac.uk

[1] D. I. Khomskii, J. Magn. Magn. Mater. **306**, 1 (2006).
[2] N. A. Spaldin and M. Fiebig, Science **309**, 391 (2005).
[3] S.-W. Cheong and M. Mostovoy, Nat. Mater. **6**, 13 (2007).
[4] N. A. Hill, J. Phys. Chem. B **104**, 6694 (2000).
[5] H. Toyosaki, M. Kawasaki, and Y. Tokura, Appl. Phys. Lett. **93**, 072507 (2008).
[6] J. Ko and C. T. Prewitt, Phys. Chem. Miner. **15**, 355 (1988).
[7] N. L. Ross, J. Ko, and C. T. Prewitt, Phys. Chem. Miner. **16**, 621 (1989).
[8] C. J. Fennie, Phys. Rev. Lett. **100**, 167203 (2008).
[9] T. Varga, A. Kumar, E. Vlahos, S. Denev, M. Park, S. Hong, T. Sanehira, Y. Wang, C. J. Fennie, S. K. Streiffer, X. Ke, P. Schiffer, V. Gopalan, and J. F. Mitchell, Phys. Rev. Lett. **103**, 047601 (2009).
[10] A. Aimi, T. Katsumata, D. Mori, D. Fu, M. Itoh, T. Kyomen, K. Hiraki, T. Takahashi, and Y. Inaguma, Inorg. Chem. **50**, 6392 (2011).
[11] M. Markkula, A. M. Arevalo-Lopez, A. Kusmartseva, J. A. Rodgers, C. Ritter, H. Wu, and J. P. Attfield, Phys. Rev. B **84**, 094450 (2011).
[12] L. C. Chapon, P. Manuel, P. G. Radaelli, C. Benson, L. Perrot, S. Ansell, N. Fhodes, D. Raspino, D. Duxbury, E. Spill, and J. Norris, Neutron News **22**, 22 (2011).
[13] Y. Syono, S. Akimoto, Y. Ishikawa, and Y. Endoh, J. Phys. Chem. Solids **30**, 1665 (1969).
[14] J. Rodriguez-Carvajal, Physica B **192**, 55 (1993).
[15] M. Markkula, A. M. Arevalo-Lopez, and J. P. Attfield, Phys. Rev. B **86**, 134401 (2012).
[16] C. G. Shull, E. O. Wollan, and W. C. Koehler, Phys. Rev. **84**, 912 (1951).